A Mathematical Transform to Analyze Part Surface Quality in Manufacturing [1]

Irem Y. Tumer
Research Scientist
Computational Sciences
NASA Ames Research Center
Moffett Field, CA 94035-1000
itumer@ptolemy.arc.nasa.gov

Kristin L. Wood
Associate Professor
Mechanical Engineering
The University of Texas
Austin, TX, 78712-1063
wood@mail.utexas.edu

Ilene J. Busch-Vishniac
Dean
Whiting School of Engineering
Johns Hopkins University
Baltimore, MD, 21218
ilenebv@jhu.edu

Abstract

The status of fault patterns on part surfaces can provide valuable information about the condition of a manufacturing system. Accurate detection of the part surface condition in manufacturing ensures the fault-free manufacturing of high-quality parts, as well as helping in the accurate design/redesign of machine components and manufacturing parameters. To address this problem, we introduce an alternative mathematical transform that has the potential to detect faults in manufacturing machines by decomposing signals into individual components. Specifically, the paper focuses on the decomposition of numerically-generated data using the Karhunen-Loève transform to study a variety of signals from manufacturing. The potential utility of the proposed technique is then discussed in the context of understanding a manufacturing process under constant development.

1 Production of High-Quality Surfaces

High-quality part production on a repeatable basis is a difficult task, requiring the continual monitoring of the manufacturing process, a thorough understanding of the manufacturing condition and capabilities, and a reliable means of information exchange between designers and manufacturers. An important question when manufacturing a component is how to enable the workpiece to function according to the designer's specifications and goals. The designer has a specific function in mind and the manufacturer has to make sure that the part is produced to satisfy this functionality (Whitehouse, 1994). An accurate understanding of the process variations is necessary to enable the design and manufacturing engineers to work as a team in assessing the process capabilities and part's potential functionality (Zemel and Otto, 1996).

"Part quality" in this work is directly related to the deviations on the surfaces of components produced by faults in manufacturing processes, that will affect the components' specified functionality. A "fault", for our purposes, is defined as the inability of a system to perform in an acceptable manner (Sottile and

[1] ASME Journal of Manufacturing Science and Engineering, Volume 122, No. 1, pp. 273-279. February 2000.

Holloway, 1994). Faults typically manifest themselves as variations in the system's quality output, indicated, for example, as undesirable vibrations of the machine tool, or variations in the surface profile of the final product. There are various factors that may contribute to such deviations. As a result, it becomes crucial to accurately decompose the various components of the surface and attempt to understand their nature and potential for damage to the part's quality (Sottile and Holloway, 1994).

2 Paper Focus

This work relies on the idea of "fingerprinting" the manufacturing process in order to detect and characterize all significant patterns on product surfaces, by means of mathematical techniques. In this paper, we introduce a potential tool for this purpose and present results based on numerically-generated signals. These signals represent one-dimensional profile measurements collected from manufactured surface profiles. Various fault situations are simulated in order to demonstrate the decomposition abilities of the proposed tool. The results are then discussed in the context of an application to a manufacturing process under continuous development, namely, Selective Laser Sintering.

3 Mathematical Techniques for Surface Quality Monitoring

Traditional methods to analyze one-dimensional surface measurements rely on surface characterization by means of average measures (e.g., surface roughness measures, kurtosis, etc.), time series analysis methods (e.g., ARMA parameters), and, more recently, mathematical transforms (e.g., Fourier spectrum) (Whitehouse, 1994). Techniques to decompose surface information based on the Fourier transform have become standard in manufacturing. Such a decomposition transforms the collected manufacturing data onto a new domain represented by sines and cosines, where understanding and interpretation become easier. The relative strength of each frequency component is determined by their relative amplitudes. However, these amplitudes can misrepresent the relevant features, since the real features (signatures) might be masked in the Fourier spectrum, especially in the presence of nonstationarities, which are completely smoothed out. Thus an adequate quantification of the relative significance of the various frequency components is not possible.

To overcome the shortcomings of traditional methods in face of the increasing expectations from manufacturing processes, ongoing research aims at finding more suitable methods to analyze signals with a multitude of different characteristics. Some of these methods involve more advanced mathematical transforms, such as the Wigner-Ville transform, wavelet transforms, higher-order spectral transforms, etc. (Berry, 1991; Fackrell et al., 1994; Geng and Qu, 1994; Jones, 1994; Rao et al., 1990; Rohrbaugh, 1993). The Wigner-Ville transformation typically introduces redundant features when dealing with multicomponent signals (Rohrbaugh, 1993; Whitehouse and Zheng, 1992). This redundancy tends to obscure the significant fault features. De-

spite of its many strengths, in the standard formulation of the wavelet transform, it is difficult to attribute physical meaning to the features (wavelet coefficients) extracted from the wavelet decomposition (Kasashima et al., 1995; Lee et al., 1998; Geng and Qu, 1994; Ladd, 1995). Using higher-order spectral transforms, it is often difficult to isolate and interpret the features corresponding to nonstationary signals (Barker et al., 1993; Fackrell et al., 1994). In addition to these transforms, there exist other transforms, including Gabor transforms, Walsh transforms, and Haar transforms (Kozek, 1993; Whitehouse, 1994), but these are simply extensions of the Fourier, Wigner-Ville, and wavelet transforms, so their utility is similar.

While there is an increasing number of research efforts in showing the applicability of such advanced mathematical techniques, their implementation in manufacturing practice remains difficult. This problem is mainly due to the difficulty in interpreting the information from these transforms and the inability to provide a clear and easy to understand picture of the manufacturing data. In order to bridge manufacturing and design, it is crucial that a method that is easily implementable in practice be developed.

4 Karhunen-Loève Transform

As an alternative to the methods for use in signal monitoring, we propose the use of an interesting mathematical transform, namely, the Karhunen-Loève (KL) transform. The KL transform decomposes signals into individual components in the form of empirical basis functions that contain the significant variations in the original data. The transform has been used in many applications, ranging from the recognition of faces to the detection of coherent speech components (Algazi et al., 1993; Ball et al., 1991; Graham et al., 1993; Grigoriev et al., 1998; Martin et al., 1996; Sirovich and Keefe, 1987). However, the application of the transform in representing and identifying fault patterns in manufacturing has been rare. The reluctance in using the transform is partially due to the perceived difficulty in attributing physical significance to the outputs.

The KL transform is studied in this work because of its inherent ability to obtain an accurate decomposition of signals into dominant individual components. The power of the KL transform stems from the fact that it can be applied to any type of signal, whether deterministic, stochastic, stationary, or nonstationary, without prior knowledge of the characteristics of the fault patterns (Fukunaga, 1990; Kozek, 1993; Therrien, 1992). In addition, the KL transform acts as a filter which increases the signal-to-noise ratio; the dominant components correspond to the coherent features, whereas the low-significance components contain the stochastic nature of the data. Reconstruction of estimates of the original data have increased signal-to-noise ratios when the low-significance components are omitted.

4.1 Mathematical Background

The mathematical background of the KL transform can be found in the literature in many different contexts. In our work, we present this background in the context of surface analysis. The signal being monitored is the surface profile of a manufactured part. A total of M "snapshots" are assumed to be collected at regular intervals to allow for continual monitoring of the state of operation. Each snapshot has a total of N sample points.

The collected profile measurements are the $\vec{P}_m$ input vectors for the KL analysis. First, the mean vector $\vec{P}_{ave} = \frac{1}{M}\sum^m \vec{P}_m$ over all M samples in the ensemble is computed; then the deviation or departure $\vec{d}_m = \vec{P}_m - \vec{P}_{ave}$ of each sample signal from the ensemble mean is computed. Next, using the deviations of the input snapshots from the mean profile, the covariance matrix is computed as follows:

$$\vec{V} = \frac{1}{M}\sum_{m=1}^{M} \vec{d}_m[\vec{d}_m]^T, \tag{1}$$

where M is the number of input vectors for the method, or snapshots of the process being monitored. The covariance matrix contains all the variation in the input data. Then, the eigenvalues and eigenvectors of the covariance matrix are computed. The eigenvectors of $\vec{V}$ are the basis functions $\vec{e}_i$ which satisfy the following eigenvector equation:

$$\vec{V}\vec{e}_i = \lambda_i \vec{e}_i. \tag{2}$$

The eigenvalues λ_i are then ordered, and the relevant features are selected by choosing the first $n < N$ dominant eigenvalues. Each original sample vector $\vec{P}_m$ is then reconstructed with lower dimensionality by adding the KL linear combination to the sample mean:

$$\vec{P}_m = \vec{P}_{ave} + \sum_{i=1}^{n} c_i \vec{e}_i, \tag{3}$$

where the coefficients c_i are computed by projecting each sample vector deviation $\vec{d}_m$ onto the basis vectors $\vec{e}_i$ from:

$$c_i = [\vec{d}_m]^T \vec{e}_i. \tag{4}$$

These coefficients represent the original data in the new domain represented by the dominant eigenvectors (basis functions). The set of coefficients over the number of snapshots for one eigenvector is called a coefficient vector.

5 Signal Decomposition with the KL Transform

We develop a series of analytical signals for the purpose of modeling multicomponent signals to show the types of fault patterns that can be detected with this technique. Multicomponent signals are defined to

be signals consisting of a combination of patterns, as opposed to "pure" signals consisting of a single signal pattern.

5.1 Numerical Signals

The "normal" state of operation is assumed to produce a multicomponent signal with two sinusoidal functions, in the form of $A_1 sin[\omega_1 j] + A_2 sin[\omega_2 j]$: one with high frequency ($\omega_1 = 0.9\ rad/sec$), small amplitude ($A_1 = 3\ mm$), and the other with low frequency ($\omega_2 = 0.2\ rad/sec$) and large amplitude ($A_2 = 6\ mm$), plus random (Gaussian) noise (zero mean and variance of 0.9). This situation illustrates a typical operation state, in which rotating components introduce fundamental sinusoidal patterns, accompanied with random noise from the machine operation or other conditions. Faults, such as bearing wear or misalignment, introduce either additional harmonics, or a change in the magnitude of the fundamental frequency components. In addition, offsets or linear trends may be introduced as a result of misalignment in the non-rotating elements.

To detect deviations from the normal state of operation, we introduce several fault conditions, summarized as follows (Tumer et al., 1997):

1. The high frequency component increases in amplitude, while the remaining patterns are the same as the normal state of operation (Faulty State 1).

2. The mean offset of the normal state of operation changes while monitoring the signal (Faulty State 2).

3. The amplitude of the low frequency component increases while monitoring the signal (Faulty State 3).

5.2 Simulation Results

$M = 30$ snaphots of a manufacturing signal are assumed to be collected over time, with $N = 256$ sampled points each. Table 1 presents the eigenvalues (Equation 2) for the normal state of operation, and the faulty states over the snapshots. We tabulate ten (out of thirty) of the eigenvalues; only a small number of these correspond to the significant eigenvectors. Note that the eigenvalues correspond to the mean-squared value of the coefficient vectors. The significance of each pattern is indicated by the magnitude of the eigenvalues. A change in the severity of a particular pattern can be indicated by a corresponding change in the significance of the eigenvalues. The significance of the resulting eigenvalues in Table 1 will be discussed in the following subsections. Notice that the eigenvalues are always listed in a descending order. Thus one cannot assume that the index i corresponds to the same eigenvector in each case. Any differences are explained in each case. Also note that, the eigenvectors corresponding to a sinusoidal component are given in pairs (e.g., Eigenvalues #1 and #2 for Normal State). This is due to the sampling procedure of a long sequence of data, which is split into multiple short sequences (representing the multiple snapshots of the manufacturing signal over time), hence introducing a phase component. As a result, a sinusoidal signal component is represented

Table 1: Eigenvalues: Normal vs. Faulty States.

Index	Normal	Faulty 1	Faulty 2	Faulty 3
1	2326.46	5296.41	6442.26	3993.21
2	2267.09	5121.70	2469.42	3450.75
3	594.20	2349.09	2121.66	598.16
4	567.13	2209.03	592.16	573.82
5	12.52	13.56	577.44	12.80
6	10.96	11.05	11.94	11.63
7	10.84	10.86	11.29	11.14
8	10.69	10.51	10.57	10.81
9	10.31	10.06	10.19	10.08
10	10.03	9.76	9.68	9.22

by a pure sinusoid, and its counterpart, shifted by a phase angle of 90 degrees, orthogonal to the first one. In the remaining, only one of the pair of eigenvectors corresponding to a sinusoidal component will be discussed (Tumer et al., 1998b).

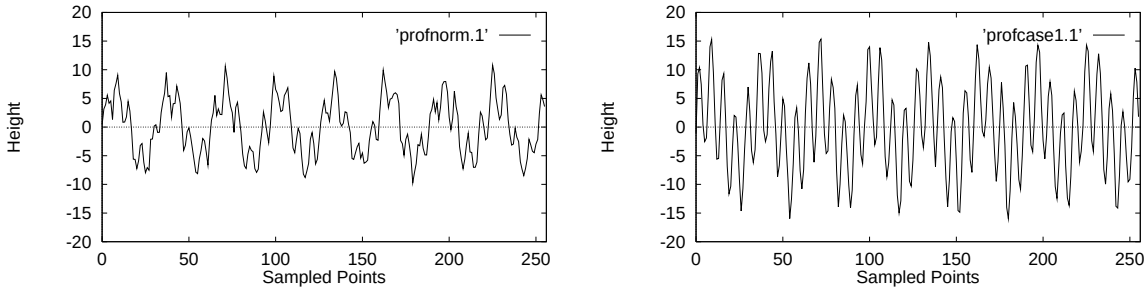

(a) Sample Profile, Normal State.

(b) Sample Profile, Faulty State 1.

Figure 1: Sample Snapshots.

5.2.1 Faulty State 1

The first example of a fault situation deals with changes in amplitudes due to a fault in the system. The multicomponent signal from the normal state of operation is contaminated by a change in one of its components. Specifically, the high frequency sinusoidal component of the signal increases in magnitude ($A_1 = 9\ mm$), while the second sinusoidal component remains unchanged. Two data sets, one from the normal state of operation, and the other from the faulty state indicating this stationary change, are collected and compared. Sample data sequences from Normal State and Faulty State 1 are shown in Figure 1.

The eigenvalues from Faulty State 1 (Figure 1(b)), compared to the Normal State (Figure 1(a)), are shown in Table 1 (recall the descending order). As in the case of the normal state of operation, for Faulty State

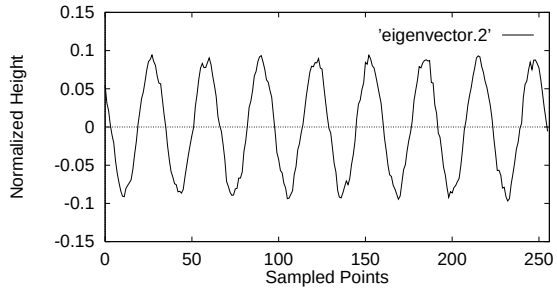

(a) Eigenvector: low frequency component.

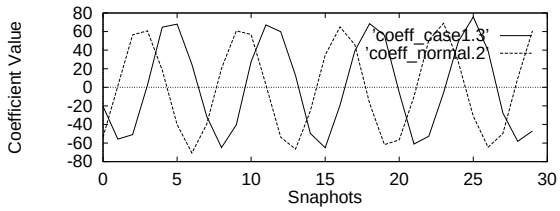

(b) Coefficient Vectors, Low-Frequency Eigenvectors.

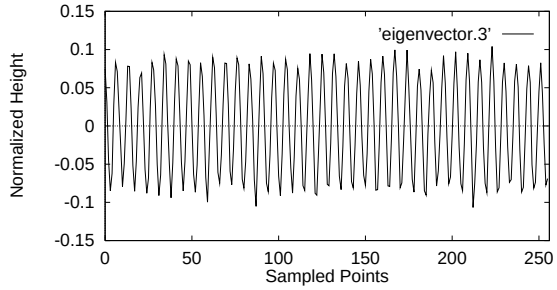

(c) Eigenvector: high frequency component.

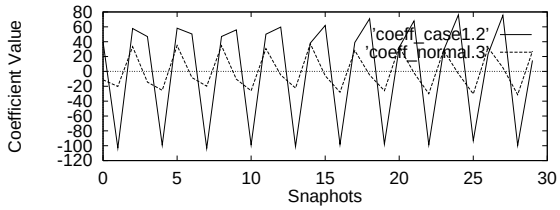

(d) Coefficient Vectors, High-Frequency Eigenvectors.

Figure 2: Normal vs. Faulty State 1.

1, we obtain four principal eigenvalues and eigenvectors (two pairs). When we increase the magnitude of the high-frequency component of the input signal, we notice that the first pair of eigenvalues, corresponding to the high-frequency component, increase in magnitude (Eigenvalues #1 and #2, Faulty State 1, Table 1), compared to the corresponding eigenvalues in the normal state of operation (Eigenvalues #3 and #4, Normal State, Table 1). Notice that the magnitudes of the eigenvalues for Faulty State 1 reflect the increase in the magnitude of the high-frequency sinusoidal component. The eigenvalues corresponding to the low-frequency component (Eigenvalues #3 and #4, Faulty State 1, Table 1) remain approximately the same in magnitude as in the normal state of operation (Eigenvalues #1 and #2, Normal State, Table 1).

These trends are more easily noticeable when we study the nature of the eigenvectors and the corresponding coefficient vectors. The main two eigenvectors from Faulty State 1, and the corresponding coefficient vectors, compared to Normal State, are shown in Figure 2. The eigenvectors show a very clear decomposition of the multicomponent signal (Figure 1(b)) into its individual components: a low-frequency sinusoidal component as indicated by the low-frequency eigenvector (Figure 2(a)), and a high-frequency sinusoidal component, indicated by the high-frequency eigenvector (Figure 2(c)). Note that the patterns of the eigenvectors are approximately the same for Normal State and Faulty State 1 (not shown). This is an expected result,

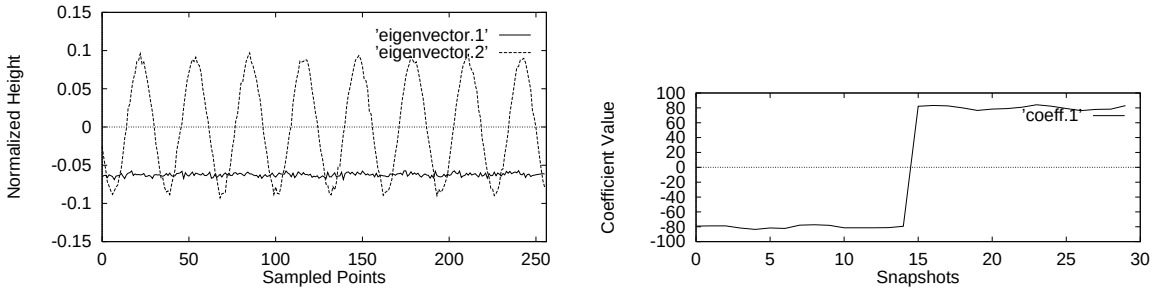

(a) Eigenvectors #1 and #2.

(b) Coefficient Vector #1.

Figure 3: Principal Eigenprofiles and Coefficient Vector for Faulty State 2.

since we are only changing the magnitude of the high-frequency sinusoidal component, and not its frequency structure. What is important in these results is that, the change in the magnitude of one of the components of the signal is detected very clearly using the coefficient vectors. Notice that the coefficient vectors corresponding to the high-frequency component show a steady increase in magnitude (Figure 2(d)). On the other hand, the coefficient vectors corresponding to the low-frequency component show no detectable magnitude change (Figure 2(b)). As a result, this change in magnitude between the two data sets is successfully detected by monitoring the coefficient vectors corresponding to the fundamental eigenvectors.

5.2.2 Faulty State 2

The next fault situation deals with the introduction of sudden changes to the monitored signal. In this case, signals from the normal state of operation are assumed to have a change in the mean offset level of the monitored signal. In these simulations, the first fifteen snapshots indicate normal status, while the next fifteen snapshots indicate an offset change.

As shown in Table 1, this fault manifests itself as an additional eigenvalue (Eigenvalue #1); the remaining eigenvalues are approximately the same as the normal state of operation (Eigenvalues #2 and #3 in Faulty State 2 compare to Eigenvalues #1 and #2 in Normal State, etc.). The simulation results, shown graphically in Figure 3(a), show that the first eigenvector simulates a linear pattern when plotted with the sinusoidal eigenvectors (for clarity, only the first sinusoidal eigenvector is shown). In addition, the coefficient vector corresponding to the first eigenvector shows the change in the mean offset very clearly, after the fifteenth snapshot (Figure 3(b)). No change is observed in the remaining eigenvectors or coefficient vectors, when compared with the normal state of operation. As a result, the additional pattern, defined by a linear function, can be detected by monitoring the occurrence of a fifth eigenvector, while its significance can be evaluated by monitoring the shape of the corresponding coefficient vector.

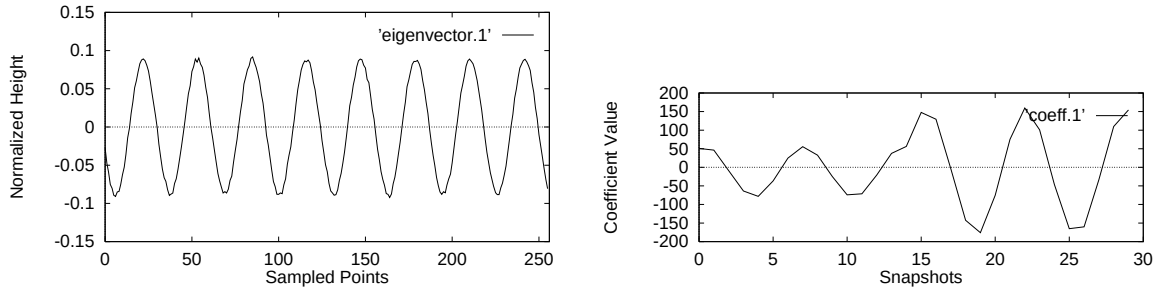

(a) Eigenvector: low frequency component.

(b) Coefficient Vector (low frequency).

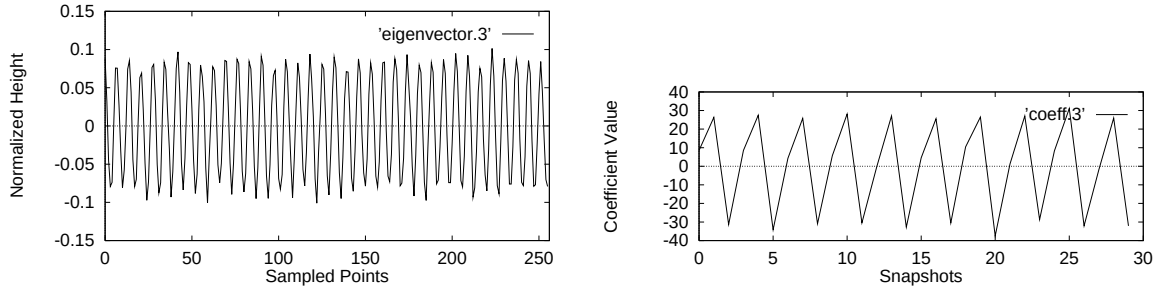

(c) Eigenvector: high frequency component.

(d) Coefficient Vector (high frequency).

Figure 4: Eigenvectors and Coefficient Vectors for Fault State 3.

5.2.3 Faulty State 3

In this third example, the low-frequency sinusoidal component suddenly undergoes a change in magnitude, while the high-frequency component remains the same. We collect a total of thirty snapshots; a change occurs during the course of monitoring the signal, hence introducing a change in the signal, after the fifteenth snapshot. The results show that, while the eigenvectors remain the same as in the normal state of operation (Figures 4(a) and 4(c)), the coefficient vectors corresponding to the low-frequency eigenvectors increase in magnitude after the fifteenth snapshot, where the change occurs (Figure 4(b)). As expected, no change is observed in the high-frequency coefficient vectors (Figure 4(d)). Also notice the increase in the eigenvalues for the first two eigenvectors (Faulty State 3) with respect to the normal state of operation, while the eigenvalues for the next two eigenvectors are approximately the same as in the normal state of operation, as shown in Table 1. As a result, the change in the data is indicated very clearly by a change in the coefficients of the faulty component in the signal.

5.2.4 Discussion of Simulation Results

The simulation results show that the KL transform has potential for detecting, extracting, and monitoring fault patterns on surface profiles. First, the KL transform successfully decomposes high-dimensional and multicomponent signals into fundamental patterns (eigenvectors). Furthermore, changes in these fundamental patterns are successfully reflected in the corresponding coefficient vectors. The introduction of additional patterns is also detected as additional fundamental patterns. For example, for Faulty State 2, the KL transform successfully decomposes the signal into its individual patterns, i.e., two sinusoids and a linear pattern. Additional patterns can be similarly detected by means of additional eigenvalues and eigenvectors (e.g., a third sinusoidal component in the original data is detected as an added eigenvector pair, decomposed clearly).

Monitoring of the offset change is performed by detecting an additional eigenvector and studying the change in the corresponding coefficient vector. In addition, the change in the offset level is reflected in the relevant coefficient vector, hence allowing its effective monitoring. A linear trend with increasing slope can be similarly detected as a linear eigenfunction, and, monitored with the coefficient vector, indicating the change in slope (Tumer et al., 1997; Tumer et al., 1998b), as shown in the last example. In Faulty State 3, the change in the magnitude of the sinusoidal patterns is successfully reflected in the relevant coefficient vectors, while no additional patterns are extracted.

Finally, coherent modes are shown to be easily detectable, even in the presence of stochastic noise, which typically obscure the true information in the data. Stochastic noise is collected in the low-eigenvalue terms, and filtered from the fundamental eigenvectors. In addition, the clarity of the picture and information provided by the KL eigenvector-coefficient vector combination makes this technique a good candidate for implementation in manufacturing practice.

6 Potential Utility in Manufacturing

To demonstrate the potential utility of the KL-based decomposition technique, a number of sample profiles from a manufacturing process are studied next. To show the clarity of information provided by the KL transformation, the following example concentrates on the decomposition abilities of the proposed technique.

6.1 Quality of Parts from Selective Laser Sintering

The manufacturing process under study is Selective Laser Sintering (Jacobs, 1992). Selective Laser Sintering (SLS) is a layered-manufacturing process where thin layers of powder are successively scanned to shape by means of a laser and galvanometer mirrors. Roller and piston mechanisms are used to deposit and

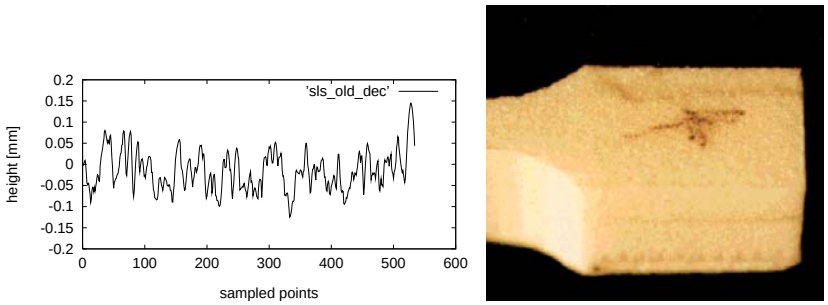

Figure 5: Surface Measurement of Part #1.

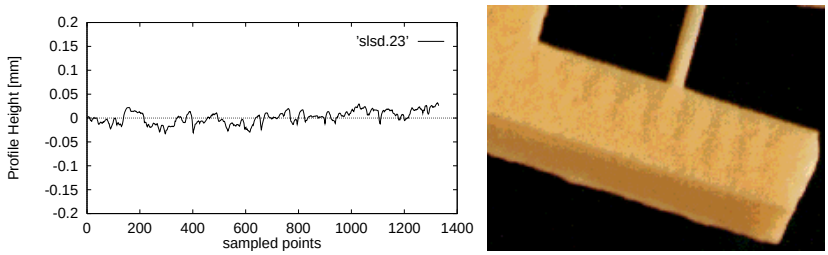

(a) Surface Structure.

Figure 6: Surface Measurement of Part #2.

spread each layer of powder on a powder bed.

One of the main concerns in this layered-manufacturing process is the ability to obtain accurate parts on a repeatable basis. Any of the components and/or parameters of the Selective Laser Sintering machine may result in undesirable fault patterns on part surfaces. As a result, it is important to understand the surface characteristics of parts produced using this process (Tumer et al., 1998a).

6.2 Improving the Surfaces of SLS Parts Using KL

We first investigate surfaces of parts built using a polycarbonate powder, shown in Figure 5. These surfaces indicate a "rough-to-touch" structure, which the designers would like to eliminate. Analysis of these surface profiles using the KL transform reveals a predominantly stochastic structure, without any coherent structures revealed.

Figure 6(a) shows a part produced using a powder with smaller particle size. The corresponding surface profile shows an improvement over the previous part profile. The surface roughness has been reduced to an average value of 10 *microns*, and the part surface is no longer rough to touch. The improvement of the surface roughness is satisfactory to the designer and the customer. However, as a consequence of the first remedial action, additional fault patterns are revealed on the new part surfaces. We next analyze the same

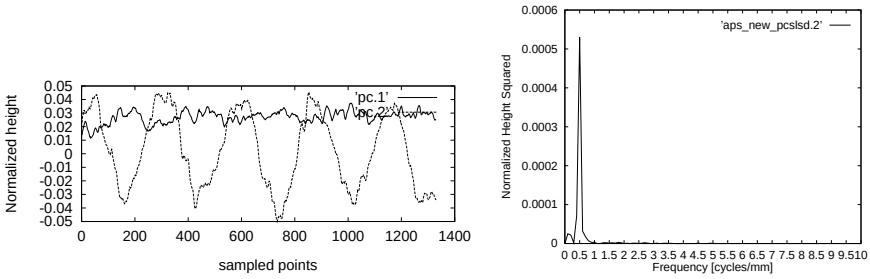

(a) Eigenvectors. **(b)** Spectrum of Eigenvector #2.

Figure 7: Karhunen-Loève Analysis of Surfaces from Part #2.

surface (Figure 6(a)) using the KL transform technique. This analysis results in two eigenvectors, which are identified as the two dominant components, shown in Figure 7(a). In particular, the sinusoidal component is clear and distinct. This provides an unambiguous way of detecting the correct frequency component corresponding to the low-frequency waveform on part surfaces, at a frequency of $f = 0.5\ cycles/mm$. The dominant frequency component is due to the nonstationary trends in the data. This nonstationary trend is isolated by means of the first KL eigenvector, shown in Figure 7(a).

The waveform at the frequency identified in Figure 7(b) corresponds to the roller chatter frequency identified from vibrational measurements. By collecting vibrational measurements from the roller mechanism, the designer can match the waveform frequency to the roller chatter frequency. Monitoring both submechanisms will provide a means to assure that the magnitude of the surface fault pattern is below an unacceptable threshold. The threshold levels can be set based on customer specifications. When this threshold is exceeded, the fault pattern is deemed severe; the remedial action taken by the designer is to look into ways of redesigning the roller mechanism. This systematic surface analysis procedure provides a means to understand the potential fault mechanisms in the manufacturing process under investigation. This information is conveyed to the designer, who then implements remedial measures to prevent or eliminate the potential problems. This analysis can be carried out for different surfaces to determine and categorize the different fault mechanisms affecting surface quality during part production (Tumer et al., 1998a).

7 Conclusions

This paper presents a potential fault detection method to tie the design and manufacturing fields more effectively. A fault detection and monitoring method based on the Karhunen-Loève (KL) transform is presented, where the eigenvectors and the corresponding coefficient vectors are proposed as an effective means of detecting faults in manufacturing. The information represented by this technique is clear and easy

to interpret. The unambiguous detection of faults in manufacturing is essential to help designers in designing the manufacturing machine and/or choosing machine parameters to improve the precision of parts produced from manufacturing machines. Essential knowledge gained from such mathematical detection tools can be used to understand and redesign a manufacturing process.

In particular, we present a systematic investigation of signal decomposition using the Karhunen-Loève transform. Numerical data is generated to model manufacturing signals and possible changes indicative of faults. By illustrating the decomposability of models of manufacturing signals, we show that the KL transform results in clearly interpretable features. These KL features, a combination of KL eigenvectors and coefficients, effectively identify various signal components and the nature of changes in each. As a result, we show that the KL transform can be extended to the detection and monitoring of faults in manufacturing, with a promising potential to be implemented in manufacturing practice. An example in manufacturing is used to demonstrate the potential of the KL-based detection technique in achieving our goals. Specifically, surfaces of parts from a Selective Laser Sintering process are analyzed with the KL-based detection technique. A design and manufacturing methodology incorporating the KL-based detection method with the design and redesign of manufacturing machines and processes is currently being developed by the authors.

Acknowledgement This material is based on work supported, in part, by the National Science Foundation, Grant No. DDM-9111372; an NSF Young Investigator Award; by a research grant from TARP; plus research grants from Ford Motor Company, Texas Instruments, and Desktop Manufacturing Inc., and the June and Gene Gillis Endowed Faculty Fellowship in Manufacturing.

References

Algazi, V., Brown, K., and Ready, M. (1993). Transform representation of the spectra of acoustic speech segments with applications, Part I: General approach and application to speech recognition. *IEEE Transactions on Speech and Audio Processing*, 1(2):180–195.

Ball, K., Sirovich, L., and Keefe, L. (1991). Dynamical eigenfunction decomposition of turbulent channel flow. *International Journal for Numerical Methods in Fluids*, 12:585–604.

Barker, R., Klutke, G., and Hinich, M. (1993). Monitoring rotating tool wear using higher-order spectral features. *Journal of Engineering for Industry*, 115:23–29.

Berry, J. E. (1991). How to track rolling element bearing health with vibration signature analysis. *Sound and Vibration*, pages 24–35.

Fackrell, J., White, P., and Hammond, J. (1994). Bispectral analysis of periodic signals in noise: theory, interpretation, and condition monitoring. In *EUSIPCO'94*, Edinburgh, UK.

Fukunaga, K. (1990). *Introduction to Statistical Pattern Recognition*. Academic Press, New York, NY.

Geng, Z. and Qu, L. (1994). Vibrational diagnosis of machine parts using the wavelet packet technique. *British Journal of Non-Destructive Testing*, 36(1):11–15.

Graham, M., Lane, S., and Luss, D. (1993). Proper orthogonal decomposition analysis of spatiotemporal temperature patterns. *Journal of Physical Chemistry*, 97(4):889–894.

Grigoriev, A., Chizhik, S., and Myshkin, N. (1998). Texture classification of engineering surfaces with nanoscale roughness. *International Journal of Machine Tool & Manufacture*, 38(5-6):719–724.

Jacobs, P. (1992). *Rapid Prototyping and Manufacturing: Fundamentals of StereoLithography*. Society of Manufacturing Engineers, New York.

Jones, R. M. (1994). A guide to the interpretation of machinery vibration measurements, Part I. *Sound and Vibration*, pages 24–35.

Kasashima, N., Ruiz, G. H., and Taniguchi, N. (1995). Online failure detection in face milling using discrete wavelet transform. *Annals of the CIRP*, 44(1):483–487.

Kozek, W. (1993). Matched generalized gabor expansion of nonstationary processes. In *The Twenty Seventh Asilomar Conference on Signals, Systems, & Computers*, volume 1, pages 499–503.

Ladd, M. D. (1995). *Detection of Machinery Faults in Noise Using Wavelet Transform Techniques*. PhD thesis, The University of Texas, Austin, Tx.

Lee, S.-H., Zahouani, H., Caterini, R., and Mathia, T. (1998). Morphological characterization of engineerd surfaces by wavelet transform. *International Journal of Machine Tool & Manufacture*, 38(5-6):581–589.

Martin, E., Morris, A., and Zhang, J. (1996). Process performance monitoring using multivariate statistical process control. In *IEE Proceedings on Control Theory Applications*, volume 143:2.

Rao, P., Taylor, F., and Harrison, G. (1990). Real-time monitoring of vibration using the wigner distribution. *Sound and Vibration*, pages 22–25.

Rohrbaugh, R. A. (1993). Application of time-frequency analysis to machinery condition assessment. In *The twenty-seventh Asilomar Conference on Signals, Systems, & Computers*, volume 2, pages 1455–1458.

Sirovich, L. and Keefe, L. (1987). Low-dimensional procedure for the characterization of human faces. *Journal of the Optical Society of America*, 4(3):519–524.

Sottile, J. and Holloway, L. E. (1994). An overview of fault monitoring and diagnosis in mining equipment. *IEEE Transactions on Industry Applications*, 30(5):1326–1332.

Therrien, C. (1992). *Discrete Random Signals and Statistical Signal Processing*. Prentice Hall, Englewood Cliffs, NJ.

Tumer, I., Thompson, D., Wood, K., and Crawford, R. (1998a). Characterization of surface fault patterns with application to a layered manufacturing process. *Journal of Manufacturing Systems*, 17(1):23–36.

Tumer, I., Wood, K., and Busch-Vishniac, I. (1997). Improving manufacturing precision using the Karhunen-Loève transform. In *1997 ASME Design for Manufacturing Conference, Integrated Design Symposium*, volume DETC97-DFM4347 (cdrom).

Tumer, I., Wood, K., and Busch-Vishniac, I. (1998b). Condition monitoring methodology for manufacturing and design. In *1998 ASME Design for Manufacturing Conference*, volume DETC98-DFM5724 (cdrom).

Whitehouse, D. (1994). *Handbook of Surface Metrology*. Institute of Physics Publishing, Bristol, UK.

Whitehouse, D. and Zheng, K. (1992). The use of dual space-frequency functions in machine tool monitoring. *Measurement Science and Technology*, 3:796–808.

Zemel, M. and Otto, K. (1996). Use of injection molding simulation to assess critical dimensions and assign tolerances. In *The 1996 ASME Design Engineering Technical Conference and Computers in Engineering Conference*, volume DETC96-DFM1277 (cdrom).